Coumarin Based Highly Selective 'Turn-On' Fluorescent Probe for Ascorbic Acid: Single Crystal X-Ray Structure and Cell Staining Properties

Dr. Subarna Guha

Faculty of Chemistry, Central Institute of Plastic Engineering and Technology, Haldia, West Bengal, India

Abstract:- **A vanillin-coumarin hybrid molecule, 6E)-6-(4-hydroxy-3-methoxybenzylideneamino)-2H-chromen-2-one (VC) has been found to interact with ascorbic acid (AA) very selectively via intermolecular H-bond formation resulting a 8 fold enhancement of its fluorescence intensity. Interaction has been monitored by different spectroscopic techniques like ^{1}H NMR, QTOF–MS ES^{+} and FTIR analysis. Structure of VC has been confirmed by single crystal X-ray structure analysis. In DMSO/water (1:4, v/v) at pH 7.4, the method is linear up to 14 µM of AA and can detect as low as 0.5 µM AA. Interference from common cations, anions and some common pharmaceutical compounds with close structural resemblance is negligible. VC can detect intracellular AA in living cells very efficiently.**

Keywords: **Turn-on fluorescence, ascorbic acid, coumarin, living cell imaging.**

I. INTRODUCTION

Use of fluorescence technique for trace level detection[1-2] of analyte has become very popular and the volume of research work in this field is exponentially rising. L-Ascorbic acid (**AA**), a water-soluble vitamin C, is widely distributed in fruits and vegetables, and plays an important role in human metabolism as a free-radical scavenger.[5] Radical induced disease[6] such as cancer and Parkinson's disease is prevented by it. Deficiency of this acid causes scurvy disease. It also plays many important biological roles[7-8] e.g. a vital role in disease prevention. It also used some commercial soft drink beverages, pharmaceutical formulations, and cosmetic applications.[9] Due to the above importance of **AA**, its determination in solutions is very important.

Recently, **AA** has attracted considerable attention for its use in modern cancer therapy.[10-11] A wide variety of analytical techniques is available for the determination of **AA**, including as titrimetric analysis, spectroscopy, chromatography, and electroanalysis.[12-13] So far, various **AA** analytical procedures have been reported, including HPLC,[14] spectrometric,[15] chemiluminescence,[16-18] capillaryelectrophoresis,[19] modified electrodes,[20-22] electrochemical methods[23] chemiluminescence,[24] atomic absorption spectrometry,[25] luminescent[26] and so on. Although, very few **AA** selective fluorescence sensors have so far been reported, [27-30] and the majority of them require a tedious synthetic methodology. Most of these methods lack selectivity, sensitivity and are not free from interference. Although it has become necessary to directly detect **AA** today, no fluorescence bio imaging technique has been established thus far. This has led to many limitations; for example, investigations on cellular uptake of **AA** had been restricted only to indirect techniques such as radiometric measurements of cells including radioactive **AA** or high-performance liquid chromatography–electrochemical detections of **AA** extracted from cells.[31-32] The fluorescence technique offers significant advantages over other methods for analyte monitoring inside living cells because of its nondestructive character, high sensitivity, and instantaneous response. Moreover, if a fluorescent chemosensor with low fluorescence intensity (off-type) shows marked enhancement in fluorescence intensity (on-type) in the presence of **AA**, it will be very sensitive for the detection of **AA** in living cells. Thus, there is a great demand for the design and easy synthesis of simple, water soluble and inexpensive **AA** selective on-type fluorescent sensors. The present report is aimed to achieve these objectives. The present sensor has some merits over other existing sensors, viz. (i) less use of organic solvent, (ii) high detection limit, (iii) one step facile synthesis of the probe, (iv)least interference from other common ions, and (v) amongst few others who performed cell imaging studies. Till date, the only one probe based on SiPc–TEMPO derivative has been used in HeLa cells[33].

From the above discussion, it is evident that the use of coumarin derivative as a fluorescent probe for trace level determination of **AA** by induced intermolecular H-bond formation of the chemosensor (**VC**) and monitoring of intracellular **AA** in infected cells might be an important area of research. Considering all these facts, herein we report the synthesis, characterizations, and cell imaging studies of a new **AA** selective fluorescent probe (**VC**) containing coumarin and vanillin units. **AA** has lactone ring with side chain –OH group so, we design this probe where lactone ring of coumarin and –OH group of vanillin moiety are present together in the Schiff base. We are currently engaged to develop low cost small molecule fluorescent probe for trace level detection of **AA** in purely aqueous or mixed aqueous organic solvent with an intention of lowering the detection limit using a greener method. In this context, here, we report the role of vanillin appended coumarin molecule (**VC**), its single crystal X-ray

structure, spectroscopic properties and interaction with **AA** with consequent changes in spectroscopic properties.

II. EXPERIMENTAL

Materials and physical measurements

Vanillin and coumarin have been purchased from Aldrich (USA) and S. D. Fine Chem. Ltd. (India) respectively. 6-aminocoumarin has been synthesized from coumarin following a literature procedure[34]. Analytical grade chemicals and spectroscopy grade solvents are used. Other chemicals were of analytical reagent grade and were used without further purification except when specified. 10 common pharmaceutical compounds *viz.* non-steroidal anti-inflammatory drug (diclofenac), analgesic and antipyretic drug (paracetamol), vitamin C (Ascorbic acid), anemia preventive drug and vitamin B_9 (Folic acid), quinolone antibiotic drug (nalidixic acid), fluoroquinolone antibiotic drug (ofloxacin and norfloxacin), nitroimidazole antibiotic drug (metronidazole), triazole antifungal drug (fluconazole), antibacterial and antiprotozoal drug (ornidazole) have been purchased from Indian Pharmaceutical Company, India. Milli–Q Millipore® 18.2 $M\Omega cm^{-1}$ water is used throughout all the experiments. All the working solutions are prepared by appropriate dilution of the stock solution with de-ionized water. Glass apparatus are kept in 4.0 $molL^{-1}$ HNO_3 overnight and cleaned with double distilled water.

^{1}HNMR spectra are recorded in DMSO-d^6 with a Bruker Advance 600 MHz using tetramethylsilane as the internal standard. Absorption and fluorescence spectra are recorded on Shimadzu Multi Spec 1501 absorption spectrophotometer and Hitachi F-4500 fluorescence spectrophotometer respectively. The slit width for both the excitation and emission studies is 5/5 nm. The fluorescence spectra have been recorded at a scan rate of 1200 nm min^{-1}. All measurements have been performed in a standard 10 mm path length quartz cell at a temperature of 25.0 ± 0.5 ºC. Mass spectra have been recorded in QTOF Micro YA 263 mass spectrometer in ESI positive mode. IR spectra have been recorded on a Perkin Elmer FTIR spectrophotometer (model: RX-1). Micro analytical data (C, H, and N) are collected on Perkin Elmer 2400 CHNS/O elemental analyzer. The fluorescence imaging system is comprised of an inverted fluorescence microscope (Leica DM 1000 LED), digital compact camera (Leica DFC 420C), and an image processor (Leica Application Suite v3.3.0). The microscope is equipped with a mercury 50 W lamp. Solutions of **AA** and **VC** have been mixed in different ratios for subsequent fluorescence measurements. A colorless prism shape crystal has been selected for crystallographic analysis using a BRUKER APPEX-II CCD single crystal X-ray diffractometer. All diffracted intensities are corrected for Lorentz and polarization effects. Absorption correction is performed with Multi-scan BRUKER SADABS. The structure has been solved by direct methods and is refined by the full-matrix least-squares on F^2 method using SHELXS97 and SHELXL97 computer programs[35]. All the non-hydrogen atoms have been refined using anisotropic atomic displacement parameters and hydrogen atoms bonded to carbon were inserted at calculated positions using a riding model. H atoms are placed at idealized positions using standard geometric criteria. The ORTEP program is used to generate the ellipsoid plot while crystal packing diagram is generated using Mercury software.

Preparation of sample solutions

The content of each tablet / capsules is carefully pulverized. A portion of this powder equivalent to contain 100 mg of the investigated drug was accurately weighed and transferred into a 100 mL volumetric flask.20 mL double-distilled water is added and sonicated for 3 minutes. The volume is made up to the mark with double-distilled water. 10 mL of this solution is diluted 100 times with double-distilled water and used as stock solution. The working solutions have been prepared from stock solution by appropriate dilution.

Working solution of **AA** is obtained by serial dilution of a 1×10^{-3} mol L^{-1} **AA** stock solution (0.0176 g of **AA** in 10 mL water). Stock solution of a 1×10^{-5} mol L^{-1} **VC** was prepared by dissolving its appropriate amount in DMSO/water (1:4, v/v).

Synthesis of (6E)-6-(4-hydroxy-3-methoxybenzylideneamino)-2H-chromen-2-one (VC)

6-Aminocoumarin (0.5 g, 3.1mmol) and vanillin (0.47 g, 3.1 mmol) are taken in dry methanol (15 mL) and refluxed for 8 h. After removal of the solvent, a yellow color compound is obtained. Yield 90%; m.p. 138±2°C; ^{1}HNMR (300MHz, Dmso-d^6) (Fig.S1), δ: 3.85 (s, 3H), 6.53(d, 1H), 6.91(d, 1H), 7.35(d, 1H), 7.38(s, 1H), 7.50(d, 1H), 7.53(d, 1H), 7.58(s, 1H), 8.07(d, 1H), 8.52(s, 1H), 9.84(s, 1H).QTOF–MS ES+, (Fig.S2)at m/z = 295.9 $[\mathbf{VC}+H]^+$. FTIR (Fig.S3)(KBr, ν, cm^{-1}) ν(CO),1699; ν(C=N), 1588;UV-Vis (Fig S4)(DMSO/water, 1:4, v/v, pH 7.4) at 298K, λ, nm (ε, $10^3 M^{-1}$ cm^{-1}), 313.50(0.213), 308.00 (0.211), 281.00(0.359), 261.00 (0.245), 234.50 (0.513), 218.00(0.283), 202.50 (0.664). Microanalytical data calculated for $C_{17}H_{13}NO_4$: C, 69.15; H, 4.44; N, 4.79, found: C, 69.08; H, 4.40; N, 4.74.

Synthesis of VC-AA adduct

10 mL DMSO solution of **AA** (0.1 g, 0.568mmol) is added slowly to a magnetically stirred 10 mL DMSO solution of **VC** (0.17 g, 0.568 mmol). The mixture is stirred in air for 15 minute to produce a clear solution. Removal of the solvent yields a deep yellow color compound. UV-Vis spectrum (Fig. S4) in DMSO/water (1:4, v/v, pH 7.4,λ, nm (ε, $10^3 M^{-1}$ cm^{-1}): 274.50 (0.556), 261.50 (0.512), 236.00 (0.701), 217.50 (0.373). QTOF-MS ES^+(Fig.S5), $[\mathbf{VC}+AA]^+$=471.26. FTIR (Fig. S6) (KBr, νcm^{-1}): ν(CO), 1669; ν(C=N), 1571. Microanalytical data calculated for $C_{23}H_{21}NO_{10}$: C, 58.60; H, 4.49; N, 2.97, found: C, 58.59; H, 4.45; N, 2.97.

III. RESULTS AND DISCUSSION

Spectral and structural characteristics

Scheme 1 shows the facile one step synthesis of the **VC**. Crystal data and structure refinement for **VC** is presented in Table S1 (**ESI**). Crystal packing diagram and ORTEP view of **VC** is presented in Fig. 1.It shows that coumarin units of two neighbouring molecules (two pairs in a unit cell) are parallel to each other. Single crystal X-ray structural details are presented in the supporting information (**ESI**). Bond lengths, bond angles and torsional angle of **VC** are presented in Table S2, Table S3 and Table S4 (**ESI**).

AA exists in equilibrium with two ketone tautomers, which are less stable than the enol form[36-40]. On the other hand, vanillin bearing a hydroxy group is expected to form intermolecular hydrogen bond with **AA** leading to rigidity of the ensemble causing fluorescence enhancement (Scheme 2). Indeed, this fact is established both from ^{1}H NMR titration and mass spectrum of the vanillin-coumarin ensemble as described in the later section.

Absorption studies. Fig.S4 illustrates the UV-Vis titration of **VC** with externally added **AA** at 25°C in DMSO/water (1:4, v/v, pH 7.4). Absorbance of **VC** at 260 nm gradually increases with increasing [**AA**] indicating the interaction of **VC** with **AA** to form an ensemble.

Emission studies. Addition of **AA** solution to the solution of **VC** results the enhancement of fluorescence intensity at 550 nm (λ_{ex} = 390 nm). Changes in the emission intensities of **VC** as a function of externally added [**AA**] (1 μM to 30 μM) are presented in Fig.2. Inset of Fig. 2 indicates that after a certain amount of externally added **AA**, there is no further change in the emission intensity of the system. It also shows the color of free **VC** solution (1 μM) and [**VC**–**AA]** ensemble under a hand held UV lamp. Fluorescence quantum yield of the [**VC-AA**] system is almost 7.6 times (0.44) than that of free **VC** (0.058) [**ESI**]. **VC** can detect as low as 0.5 μM **AA** in DMSO/water (1:4, v/v) at pH 7.4. Fig. 3 shows the plot of emission intensities of **VC** as a function of externally added [**AA**] which can be used for the determination of unknown [**AA**] in a sample. Up to 14 μM of the externally added **AA**, we observed linearity.

Job's plot (Fig.4) indicates a 1:1 stoichiometry of the complex formed between **VC** and AA which is also supported by the mass spectra of **VC-AA** complex.

Estimation of binding constant

The binding abilityof **VC** towards **AA** has been estimated following the modified Benesi-Hildebrand[41] equation $(1/\Delta F) = 1/\Delta F_{max} + (1/K[C]^n)\ (1/\Delta F_{max})$.

Where $\Delta F = (F_x - F_0)$ and $\Delta F_{max} = F_\infty - F_0$, where F_0, F_x, and F_∞ are the emission intensities of **VC** in the absence of **AA**, at an intermediate **AA** concentration, and at the concentration of complete interaction, respectively. K is the binding constant and C is the concentration of **AA** and n is the number of **AA** bound per **VC** (here, n= 1). The value of K obtained from the slope of Fig. 5 is 8.3×10^4.

Selectivity

The selectivity of **VC** for **AA** over common cations, anions and other common pharmaceutical compounds with close structural motif has been examined in DMSO/water (1:4, v/v, pH 7.4). Fig.S7 (**ESI**) indicates that only **AA** enhances the fluorescence intensity of **VC** whereas other tested pharmaceutical compounds have no significant effect. Moreover, from Fig.S8 (**ESI**) it is evident that those tested pharmaceutical compounds do not even interfere in the **AA** determination by **VC**. The effect of common cations and anions on the emission intensity of the [**VC-AA**] system has also been studied and have presented in Fig.6 and Fig.7 respectively. No significant interference is observed. Minor enhancement in fluorescence intensity has been observed in presence of Fe^{3+} and Cu^{2+} ions which has been eliminated using thiocyanate as a masking agent. SCN^- has no effect on the emission properties of the [**VC-AA**] system.

^{1}HNMR titration

In order to strengthen our conclusion based on the findings through UV-Vis and fluorescence spectroscopy, we performed ^{1}H NMR titrations by the concomitant addition of **AA** to the DMSO-d_6 solution of **VC**. Significant spectral changes were observed in the ^{1}H NMR spectra of **VC** upon addition of **AA** as shown in Fig.S9 (**ESI**). Only -OH proton of the **VC** has been shifted upfiled from 9.843 ppm to 9.767 ppm. At higher **AA** concentration, some new peaks have been observed *viz.* at 3.455, 3.734, 4.712, 4.936 and 11.059 ppm. This is due to the incorporation of **AA** unit into the system resulting formation of [**VC-AA]** ensemble. This observation is corroborated from the moderate binding constant value obtained from the fluorescence experiment. This fact has been attributed to the formation of intermolecular hydrogen bond between **VC** and **AA**.

Cell imaging

Bacillus sp. has long been used as bio-pesticide for controlling looper killer at tea plantation. These cells from 24 h culture medium have been treated with aqueous solution of **AA** (1 mg mL^{-1}) for 1h, washed with normal saline and observed under 100X fluorescence microscope after adding **VC** (Fig.8b). Fig.8a shows the control without adding **AA** but incubated with **VC**. Similarly, **VC** is very useful to stain **AA** pre-treated *Candida sp.* cells under fluorescence microscope (Fig.8d). Its corresponding control is presented in Fig.8c.

The photographs indicate that **VC** can be used to detect intracellular **AA** in living cells. **Conclusion**

Thus we have successfully developed a very simple and cheap ascorbic acid selective fluorescent probe **(VC)** whose structure has been confirmed from single-crystal X-ray structure analysis. Presence of other common pharmaceutical compounds, cations and anions do not interfere the detection

process. Detection of **AA** in living cells at physiological pH has been achieved under fluorescence microscope.

Supplementary materials

CCDC 883037 contains the structural details of the probe **VC**. The data can be obtained free of charge via http://www.ccdc.cam.ac.uk/conts/retrieving.html, or from the Cambridge Crystallographic Data Centre, 12 Union Road, Cambridge CB2 1EZ, UK; fax: (+44) 1223- 336-033; or e-mail: deposit@ccdc.cam.ac.uk. All supporting information (ESI) is available here.

ACKNOWLEDGEMENT

The authors are grateful to CIPET, Haldia for funding.

REFERENCES

[1]. A. Sahana, A. Banerjee, S. Guha, S. Lohar, A. Chattopadhyay, S. K. Mukhopadhyay and D. Das, *Analyst* 2012, **137**, 1544.
[2]. A. Banerjee, A. Sahana, S. Das, S. Lohar, S. Guha, B. Sarkar, S. K. Mukhopadhyay, A. K Mukherjee and D. Das, *Analyst* 2012, **137**, 2166.
[3]. S. Guha, S. Lohar, A. Sahana, A. Banerjee, and D. Das,*Talanta* 2012, **91**, 18.
[4]. S. Guha, S. Lohar, I. Hauli, S. K. Mukhopadhyay, and D. Das, *Talanta*2011, **85**, 1658.
[5]. R. Thangamuthu, Y.C. Wu and S.M. Chen, *Electroanalysis*, 2009, **21**, 165.
[6]. J. Du, L. Shen and J. Lu, *Anal. Chim. Acta*, 2003, **489**, 183.
[7]. O. Arrigoni and C. D. Tullio, Biochim. Biophys. Acta, Gen. Subj., 2002, **1569**, 1.
[8]. S. Englard and S. Seifter, *Annu. Rev. Nutr.*, 1986, **6**, 365.
[9]. E. Cameron and A. Campbell, *Chem.-Biol. Interact.*, 1974, **9**, 285.
[10]. E. Cameron, L. Pauling and B. Leibovitz, Cancer Res., 1979, **39**, 663.
[11]. K. Hosoya, G. Nakamura, S. Akanuma, M. Tomi and M. Tachikawa, Neurochem. Int., 2008, **52**, 1351.
[12]. V. Kmetec, J. Pharm. Biomed. Anal., 1992, **10**, 1073.
[13]. P.W. Washko, R.W. Welch, K.R. Dhariwal, Y.H. Wang, and M. Levine, *Anal. Biochem*., 1992, **204**, 1.
[14]. S.P. Arya, M. Mahajan, and P. Jain, *Anal. Chim. Acta*, 2000, **417**, 1.
[15]. O. A. Zaporozhets and E.A. Krushinskaya, *J. Anal. Chem*., 2002, **57**, 286.
[16]. X. Li and A. A. Franke, J. Chromatogr., B: Anal. Technol. Biomed. Life Sci., 2009, **877**, 853.
[17]. W. Lee, S. M. Roberts and R. F. Labbe, *Clin. Chem*., 1997, **43**, 154.
[18]. Y. Ma, M. Zhou, X. Jin, B. Zhang, H. Chen and N. Guo, *Anal. Chim. Acta*, 2002, **464**, 289.
[19]. H. Chen, R. Li, L. Lin, G. Guo and J.-M. Lin, *Talanta*, 2010, **81**, 1688.
[20]. S. Zhao, Y. Huang and Y.-M. Liu, *J. Chromatogr. A*, 2009, **1216**, 6746.
[21]. X. Sun, Y. Niu, S. Bi and S. Zhang, J. Chromatogr., B: Anal. Technol. Biomed. *Life Sci*., 2008, **870**, 46.
[22]. P.-C. Nien, P.-Y. Chen and K.-C. Ho, *Sens. Actuators B*, 2009, **140**, 58.
[23]. Y. Sato, D. Kato, O. Niwa and F. Mizutani, *Sens. Actuators B*, 2005, **108**, 617.
[24]. H. R. Zare, F. Memarzadeh, M. Mazloum-Ardakani, M. Namazian and S. M. Golabi, *Electrochim. Acta*, 2005, **50**, 3495.
[25]. M.H. Pournaghi-Azar, H. Dastangoo, R. Fadakar, *Electroanalysis*, 2010, **22**, 229.
[26]. I.B. Agater and R.A. Jewsbury, *Anal. Chim. Acta*, 1997, **356**, 289.
[27]. M. ˇZemberyova, J. Bartekova, M. Zavadska and M. ˇSiˇsolakova, *Talanta*, 2007, **71**, 1661.
[28]. H.W. Park, S.M. Alam, S.H. Lee, M.M. Karim, S.M. Wabaidur, M. Kang and J.H. Choi, *Luminescence*, 2009, **24**, 367.
[29]. C. Xia and W. Ning, Analyst, 2011, **136**, 288
[30]. H. M. Nassef, L. Civit, A. Fragoso and C. K. O'Sullivan, Analyst, 2008, **133**, 1736
[31]. N. Chauhan, J. Narang and C. S. Pundir, Analyst, 2011, **136**, 1938
[32]. C. -J. Weng, Y. -S. Jhuo, Y. -L. Chen, C. -F. Feng,C. -H. Chang,S. -W. Chen, J. -M. Yeh and Y. Wei, J. Mater. Chem., 2011, **21**, 15666
[33]. K. Ishii, K. Kubo, T. Sakurada, K. Komori and Y. Sakai, Chem. Commun., 2011, **47**, 4932.
[34]. S. Guha, S. Lohar, M. Bolte, D. A. Safin and D. Das, Spec. Lett.2012, **45**, 225.
[35]. G. M. Sheldrick, Acta Crystallogr. A 2008, **64**, 112.
[36]. K. Ishii, K. Kubo, T. Sakurada, K. Komori and Y. Sakai, Chem. Commun., 2011, **47**, 4932.
[37]. J. C. Vera, C. I. Rivas, J. Fischbarg and D. W. Golde, *Nature*, 1993, **364**, 79;
[38]. J. C. Vera, C. I. Rivas, R. H. Zhang, C. M. Farber and D. W. Golde, *Blood*, 1994, **84**, 1628.
[39]. B. S. Winkler, *Biochim. Biophys. Acta*, 1987, **925**, 258.
[40]. A. M. Bode, L. Cunningham and R. C. Rose, *Clin. Chem*., 1990, **36**, 1807.
[41]. H.A. Benesi, and J.H. Hildebrand, *J. Am. Chem. Soc*., 1949, **71**, 2703

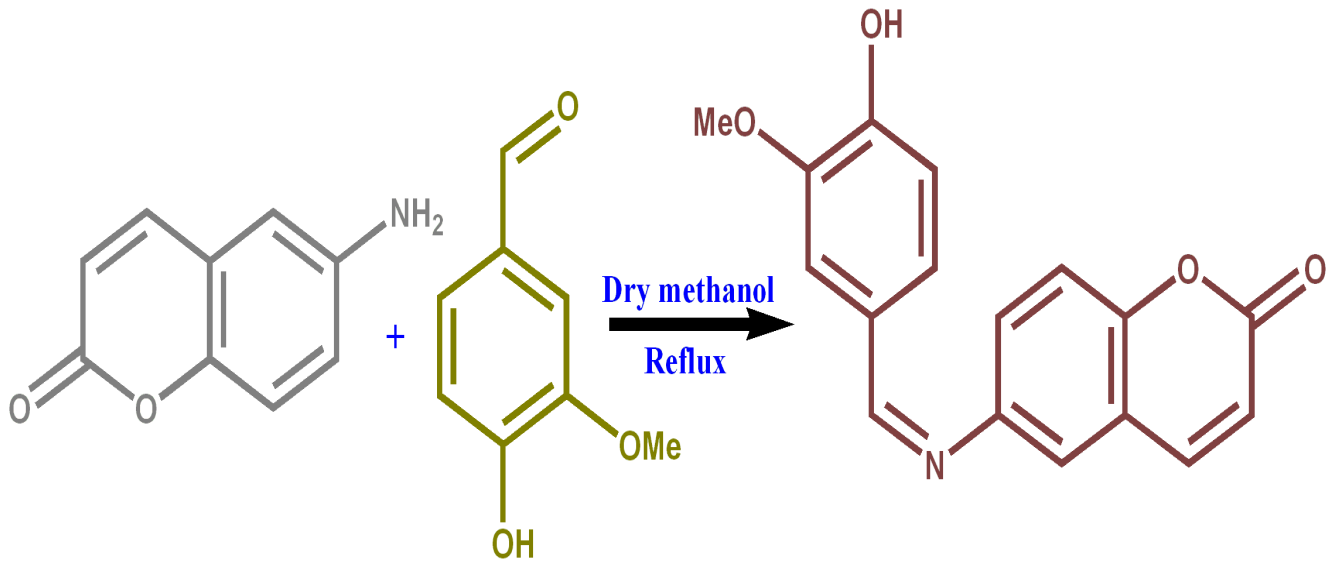

(6*E*)-6-(4-hydroxy-3-methoxybenzylideneamino)-2*H*-chromen-2-one

Scheme 1

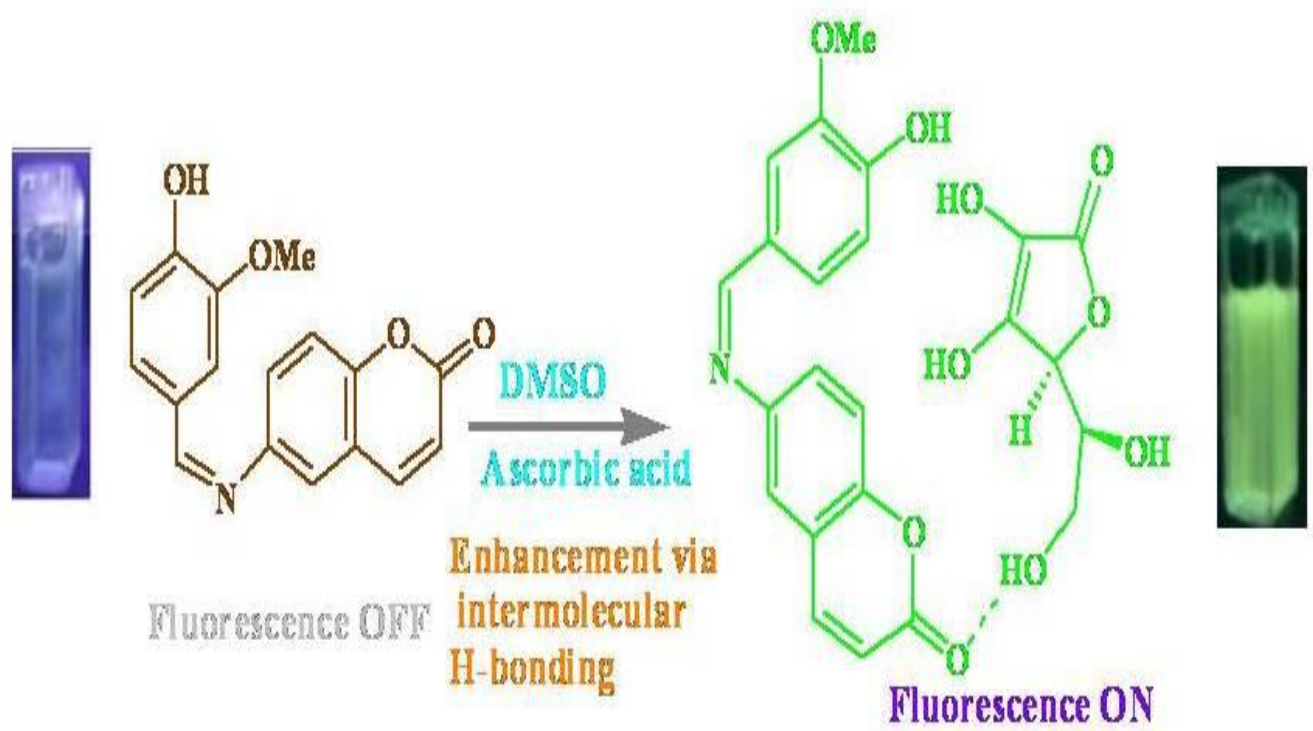

Scheme 2

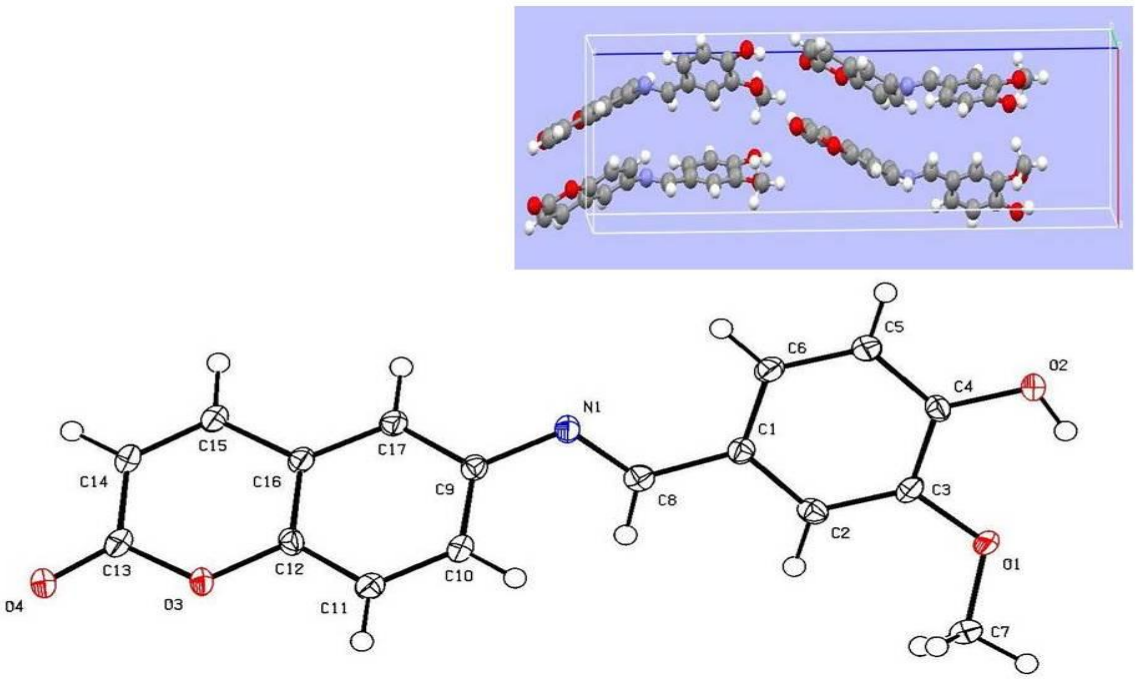
C5
C6
O2
C4
N1
C1
C15
C17
C14
C16
C9
C8
C3
C2
C13
C12
C10
O1
O4
O3
C11
C7

Fig.1

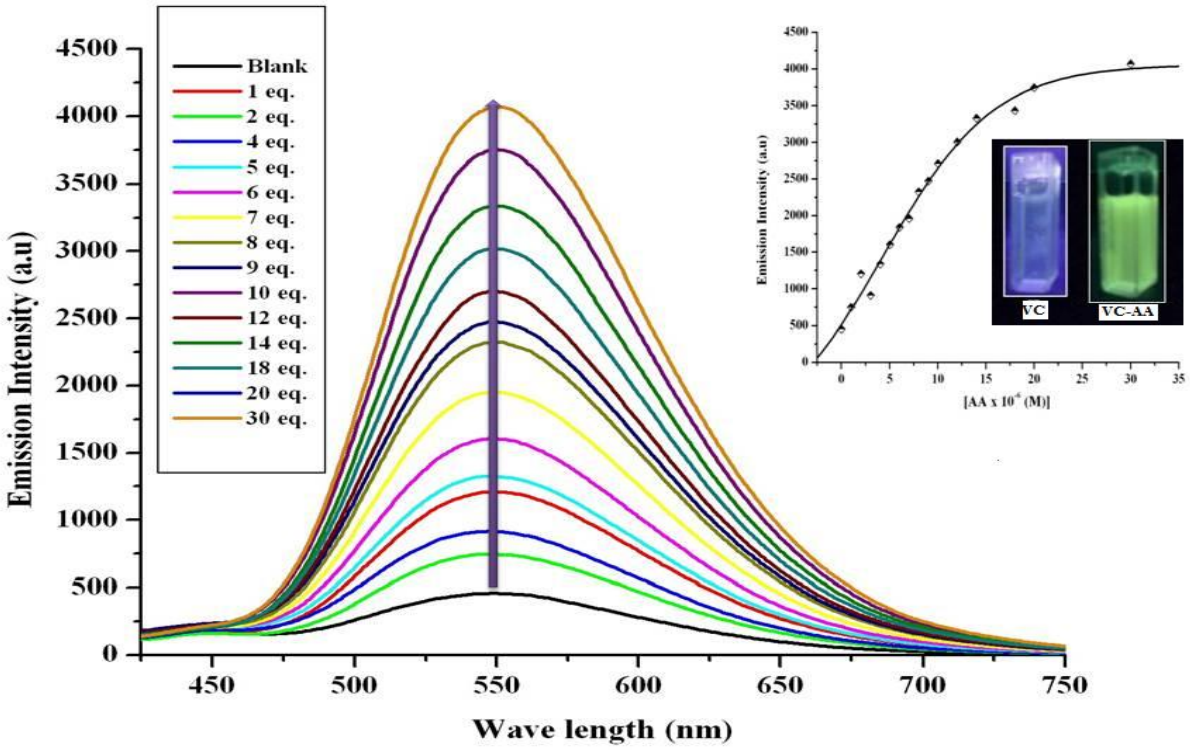
Blank
1 eq.
2 eq.
4 eq.
5 eq.
6 eq.
7 eq.
8 eq.
9 eq.
10 eq.
12 eq.
14 eq.
18 eq.
20 eq.
30 eq.
Emission Intensity (a.u)
Wave length (nm)
[AA x 10⁻⁶ (M)]
VC
VC-AA

Fig.2

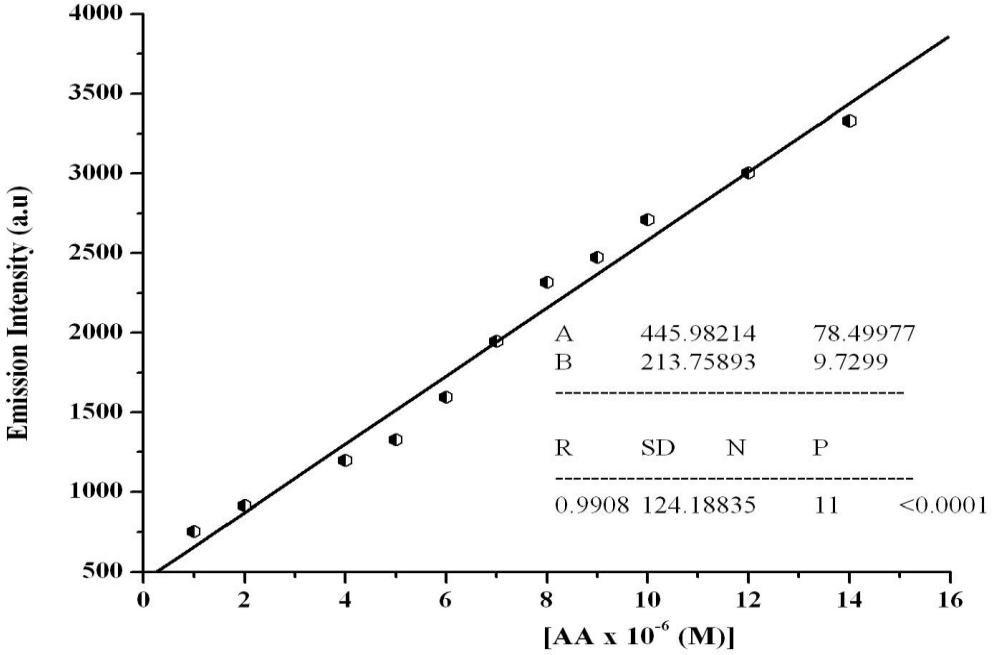
Emission Intensity (a.u)
[AA x 10^-6 (M)]
A 445.98214 78.49977
B 213.75893 9.7299
R SD N P
0.9908 124.18835 11 <0.0001

Fig.3

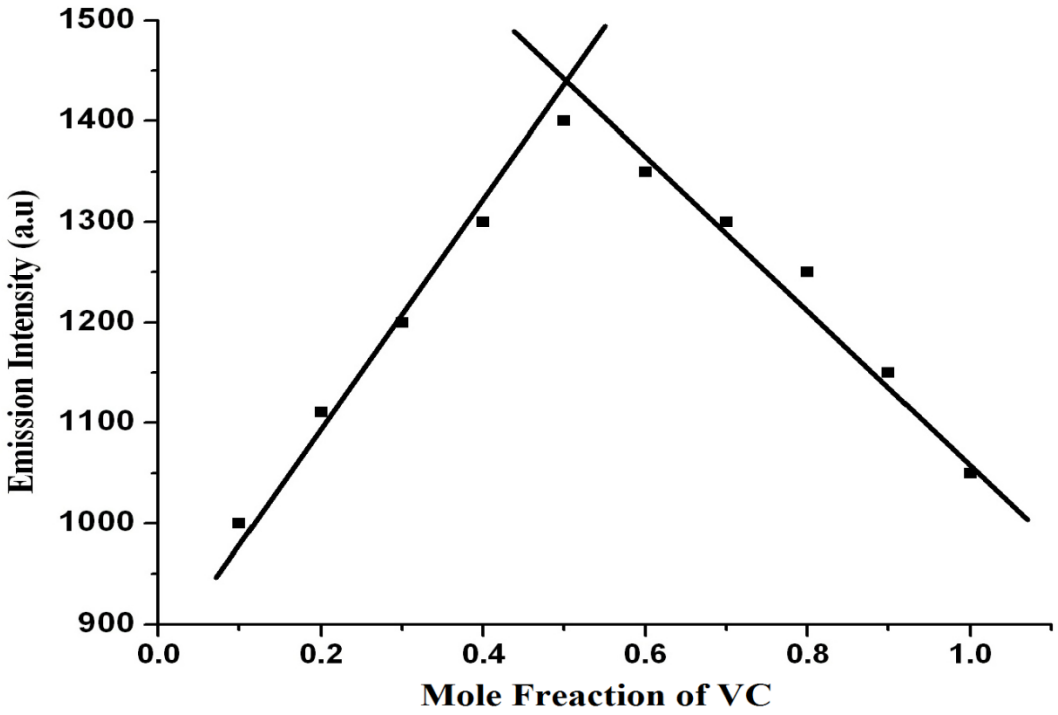
Emission Intensity (a.u)
Mole Freaction of VC

Fig.4

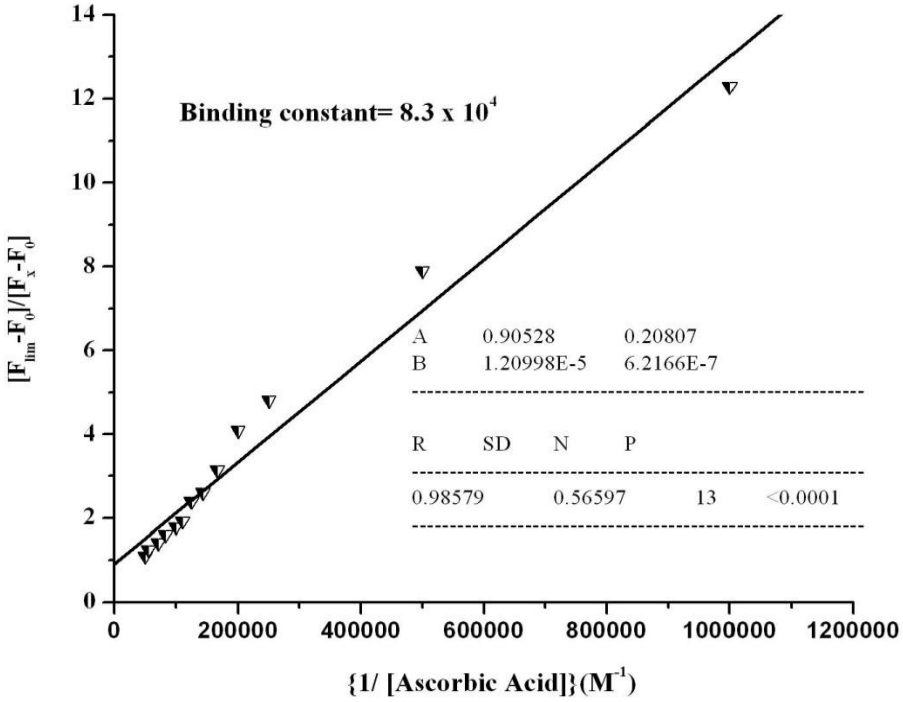
Binding constant= 8.3 x 10^4
[F_lim -F_0]/[F_x -F_0]
{1/ [Ascorbic Acid]}(M^-1)
A 0.90528 0.20807
B 1.20998E-5 6.2166E-7
R SD N P
0.98579 0.56597 13 <0.0001

Fig.5

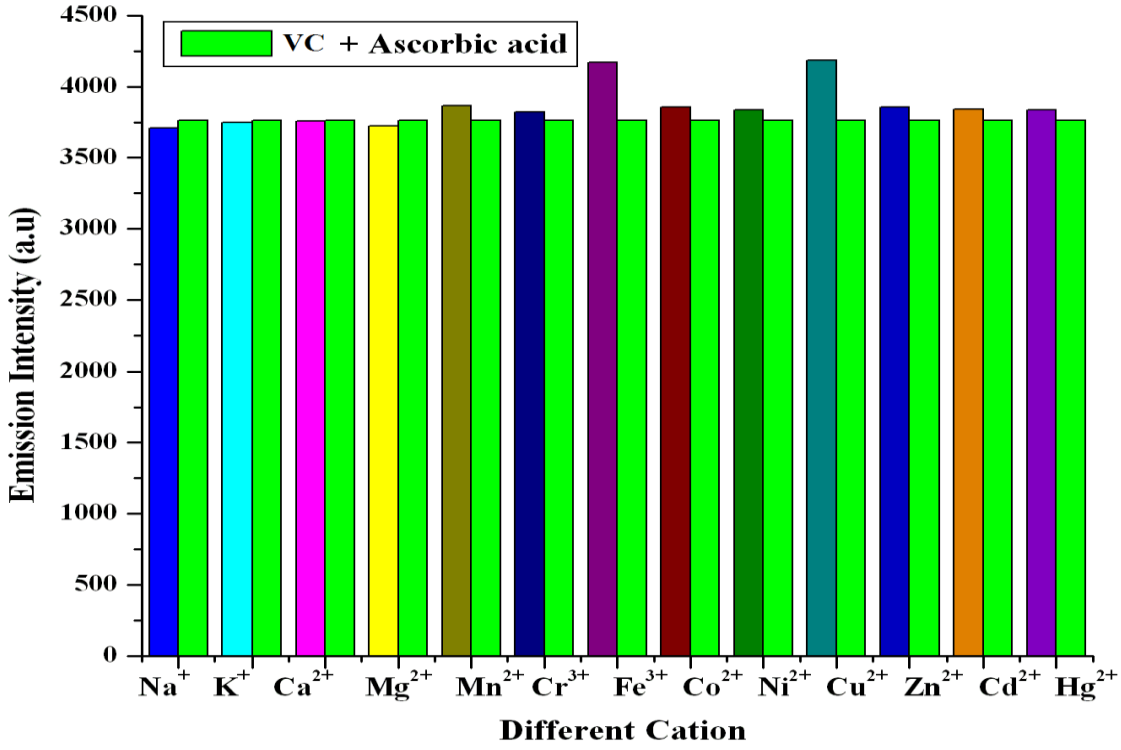
VC + Ascorbic acid
Emission Intensity (a.u)
Na+ K+ Ca2+ Mg2+ Mn2+ Cr3+ Fe3+ Co2+ Ni2+ Cu2+ Zn2+ Cd2+ Hg2+
Different Cation

Fig. 6

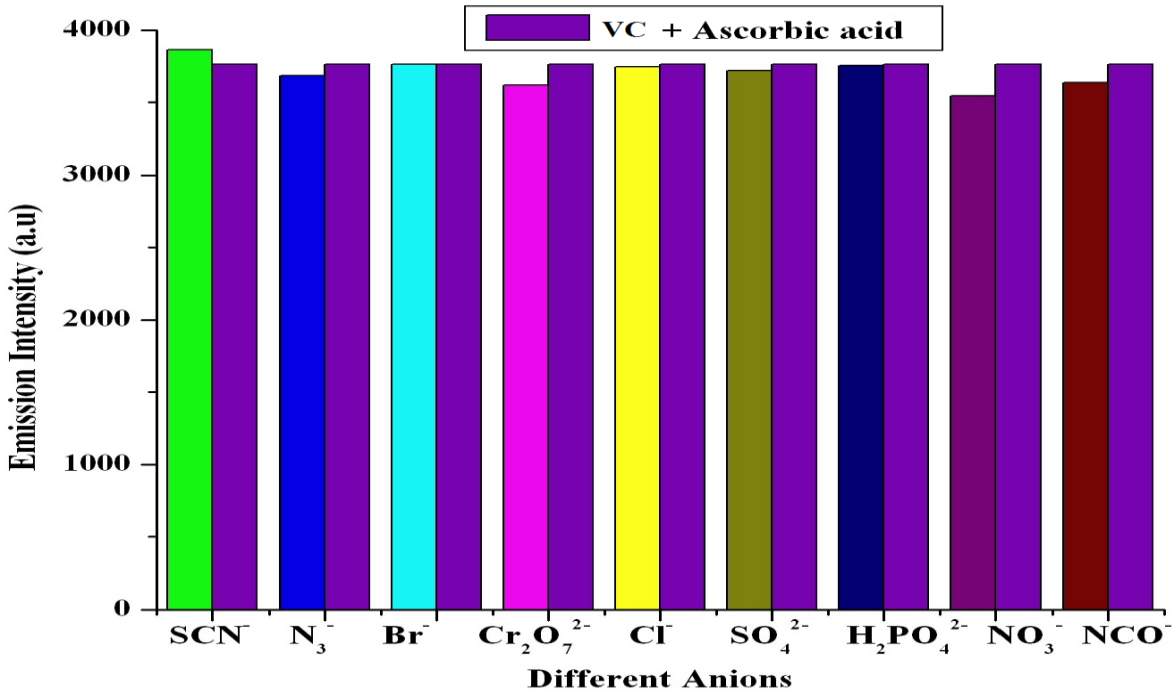
VC + Ascorbic acid
Emission Intensity (a.u)
4000
3000
2000
1000
0
SCN⁻
N₃⁻
Br⁻
Cr₂O₇²⁻
Cl⁻
SO₄²⁻
H₂PO₄²⁻
NO₃⁻
NCO⁻
Different Anions

Fig.7

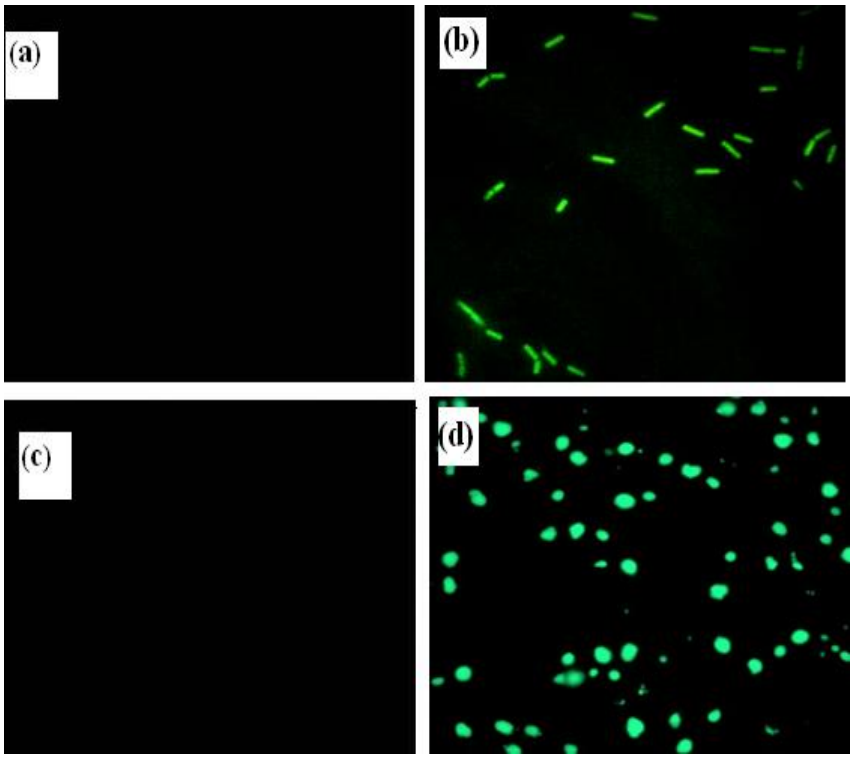
(a)
(b)
(c)
(d)

Fig.8

Legends to Figures

Scheme1. Synthesis of fluorescent sensor of (6E)-6-(4-hydroxy-3-methoxybenzylideneamino)-2H-chromen-2-one (**VC**).

Scheme2. Synthesis and probable structure of **VC**-**AA** complex.

Figure 1. Single crystal X-ray structure and packing diagram (inset) of **VC**.

Figure 2. Fluorescence spectral changes of **VC** (1 μM) up on addition of 1, 2, 4, 5, 6, 7, 8, 9, 10, 12, 14, 18, 20, 30 μM of **AA**.

Figure 3. Plot of emission intensities of **VC** (1 μM) as a function of externally added [**AA**]. Inset of Fig. 3 shows the picture of free **VC** solution (1 μM) and after addition of 1.0 equivalent **AA** under a hand held UV lamp.

Figure 4. Jobs plot for the determination of stoichiometry of [**VC**-**AA**] in DMSO/water (1:4, v/v) at pH 7.4 solution.

Figure 5. Determination of binding constant of **VC** (1 μM) with **AA** using Benesi-Hildebrand equation (fluorescence method).

Figure 6. Interference of different metal ions on the determination of [**AA**] with **VC**. [**VC**] =1 μM and [**AA**] = [foreign metal ions] = 10 μM.

Figure 7. Interference of different anions on the determination of [**AA**] with **VC**. [**VC**] =1 μM and [**AA**] = [foreign anions] = 10 μM.

Figure 8. Fluorescence microscope images of Bacillus sp.; Candida sp. (*Candida albicans)*; pollen grains of *Allamanda puberula* (Aapocynaceae) treated with **VC**. Images a, c, e, are in absence of **AA** and b, d, f, are presence of **AA** ([**VC] =** 1 μM; Incubation temperature, 40 ºC).

Supporting Information

Coumarin based highlyselective 'turn-on' fluorescent probe for ascorbic acid: Single crystal X-ray structure and cell staining properties

Subarna Guha. Central Institute of Plastic Engineering and Technology Haldia. West Bengal. India

CONTENTS

Fig. S1. ^{1}HNMR spectra of **VC**

Fig. S2. TOF MS ES (+) of **VC**

Fig. S3. FTIR spectra of **VC**

Fig.S4. UV–Vis spectra of the ligand **VC** and **VC**-**AA** complex in DMSO/water (1:4, v/v) at pH 7.4 solutions ([**VC**] =1 μM).

Fig. S5. TOF MS ES (+) of **VC**-**AA** complex

Fig. S6. FTIR spectra of **VC**- **AA** complex

Fig. S7. Emission intensities of **VC** (1 μM) in presence of different pharmaceutical compounds (1μM).

Fig.S8. Interference of different pharmaceutical compounds on the determination of [**AA**] with **VC**. [**VC**] =1 μM and [**AA**] = [pharmaceutical compounds] = 10 μM.

Fig. S9. ^{1}H NMR titrationof of the **VC**-**AA** complex

Pharmaceutical formulation

Quantum Yield Calculation

Table S1. Crystal data and structure refinement for **VC**

Table S2. Bond lengths (Å) of **VC**

Table S3. Bond angles ($^{\circ}$) of **VC**

Table S4. Tortional angles ($^{\circ}$) of **VC**

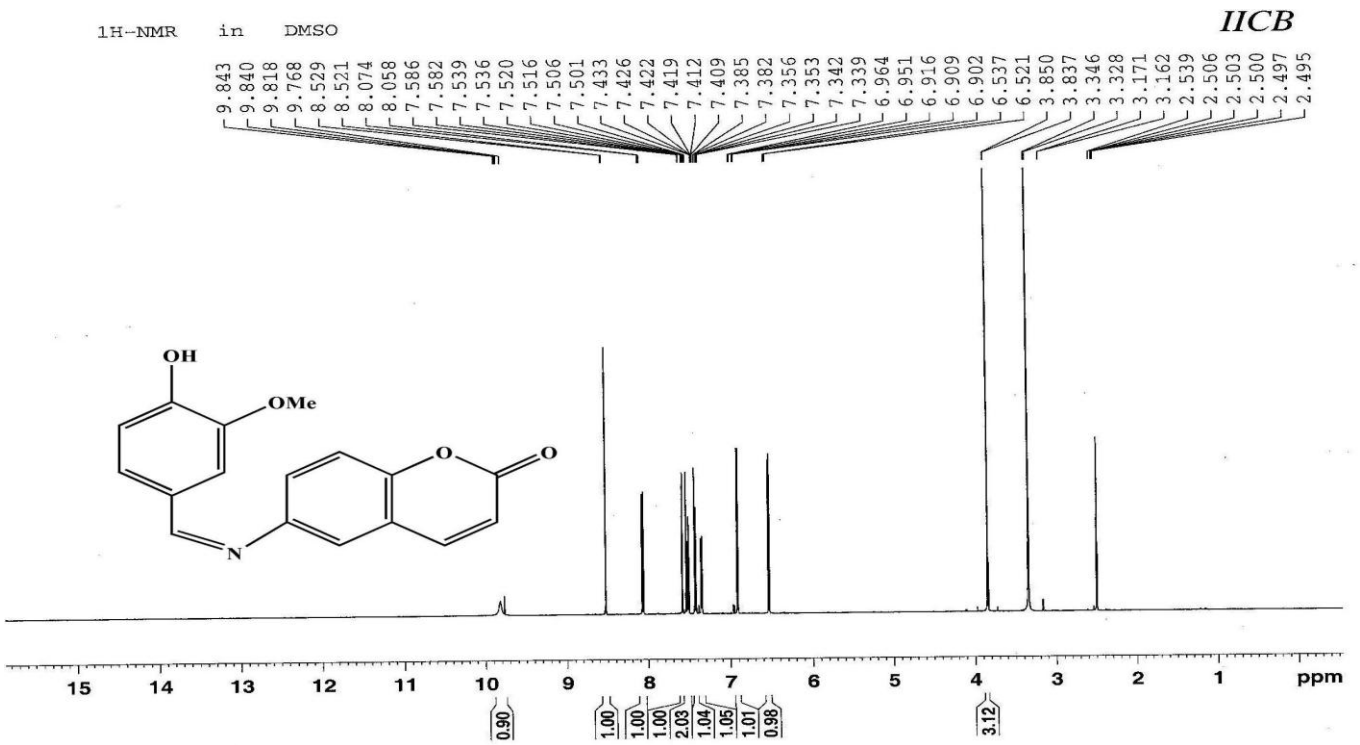
1H-NMR in DMSO
IICB
9.843
9.840
9.818
9.768
8.529
8.521
8.074
8.058
7.586
7.582
7.539
7.536
7.520
7.516
7.506
7.501
7.433
7.426
7.422
7.419
7.412
7.409
7.385
7.382
7.356
7.353
7.342
7.339
6.964
6.951
6.916
6.909
6.902
6.537
6.521
3.850
3.837
3.346
3.328
3.171
3.162
2.539
2.506
2.503
2.500
2.497
2.495
OH
OMe
O
O
N
15 14 13 12 11 10 9 8 7 6 5 4 3 2 1 ppm
0.90
1.00
1.00
1.00
2.03
1.04
1.05
1.01
0.98
3.12

Fig. S1.

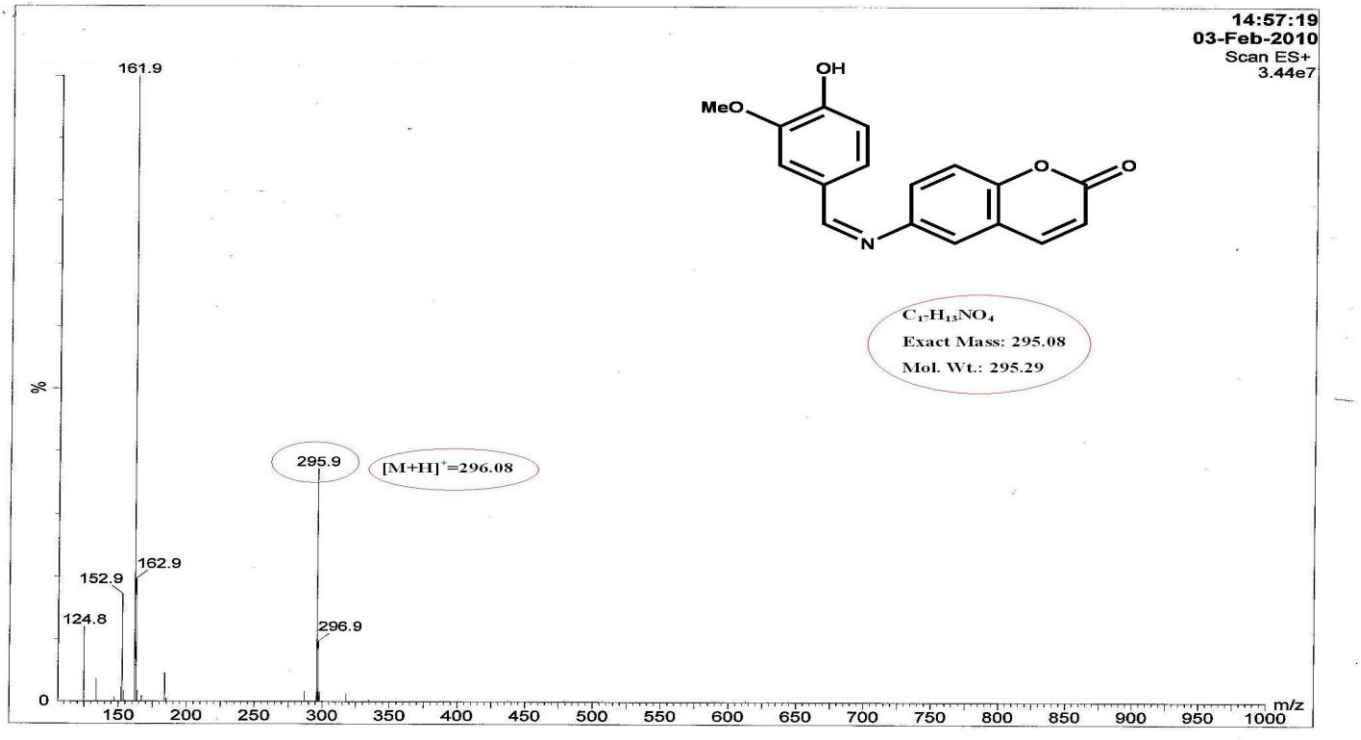
14:57:19
03-Feb-2010
Scan ES+
3.44e7
161.9
OH
MeO
O
O
N
C17H13NO4
Exact Mass: 295.08
Mol. Wt.: 295.29
%
295.9
[M+H]+=296.08
162.9
152.9
124.8
296.9
0
150 200 250 300 350 400 450 500 550 600 650 700 750 800 850 900 950 1000
m/z

Fig. S2.

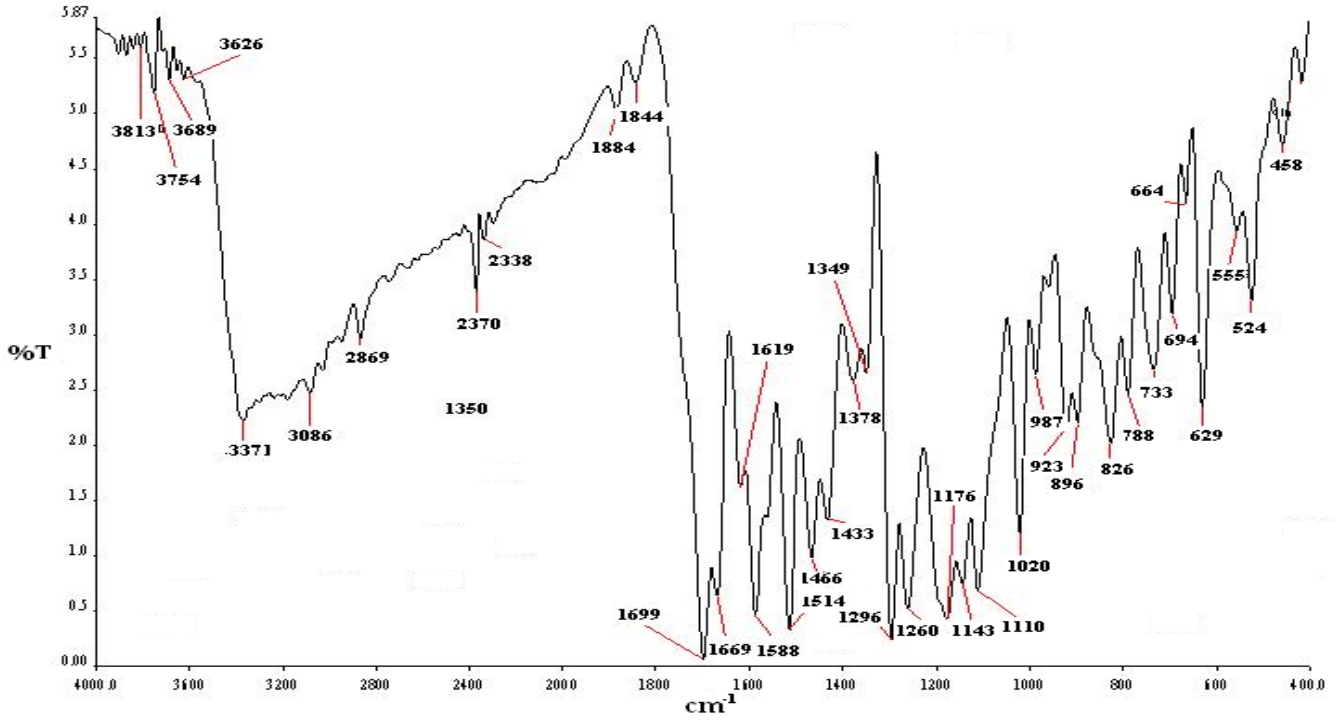
%T
cm-1
3626
3813
3689
3754
3371
3086
2869
2370
2338
1884
1844
1619
1350
1349
1378
1433
1466
1514
1699
1669
1588
1296
1260
1176
1143
1110
1020
987
923
896
826
788
733
694
664
629
555
524
458

Fig. S3.

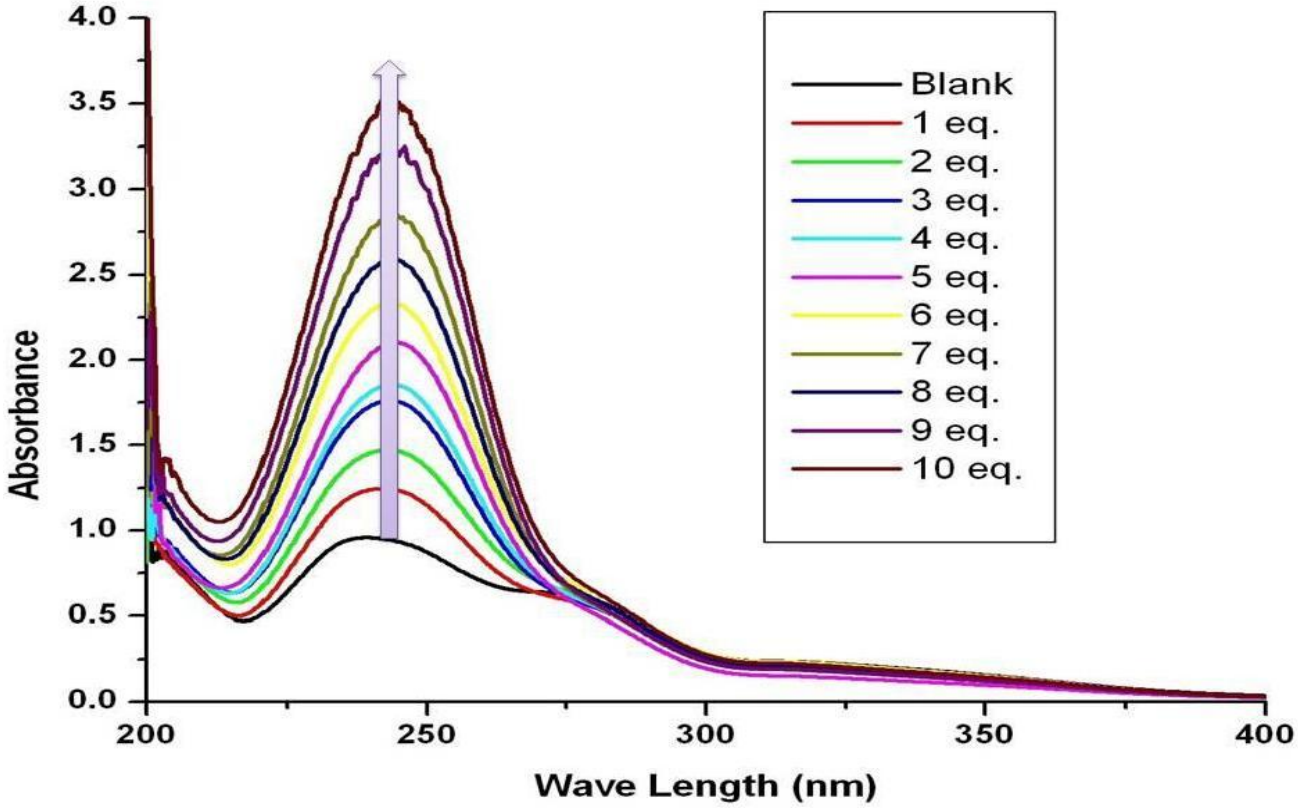
Absorbance
Wave Length (nm)
Blank
1 eq.
2 eq.
3 eq.
4 eq.
5 eq.
6 eq.
7 eq.
8 eq.
9 eq.
10 eq.

Fig. S4

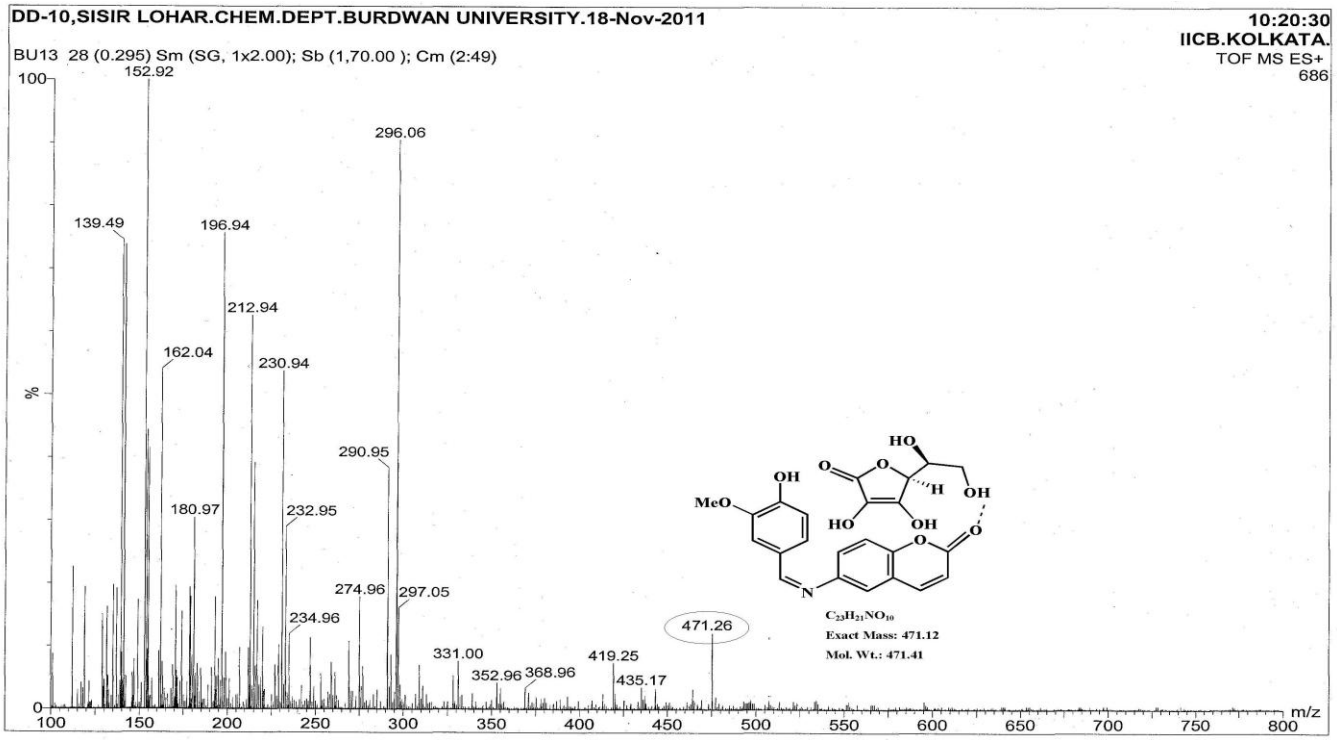
DD-10,SISIR LOHAR.CHEM.DEPT.BURDWAN UNIVERSITY.18-Nov-2011
10:20:30
BU13 28 (0.295) Sm (SG, 1x2.00); Sb (1,70.00); Cm (2:49)
IICB.KOLKATA.
TOF MS ES+
686
100
%
0
152.92
296.06
139.49
196.94
212.94
162.04
230.94
290.95
180.97
232.95
274.96
297.05
234.96
331.00
352.96
368.96
419.25
435.17
471.26
100 150 200 250 300 350 400 450 500 550 600 650 700 750 800
m/z
C23H21NO10
Exact Mass: 471.12
Mol. Wt.: 471.41

Fig. S5.

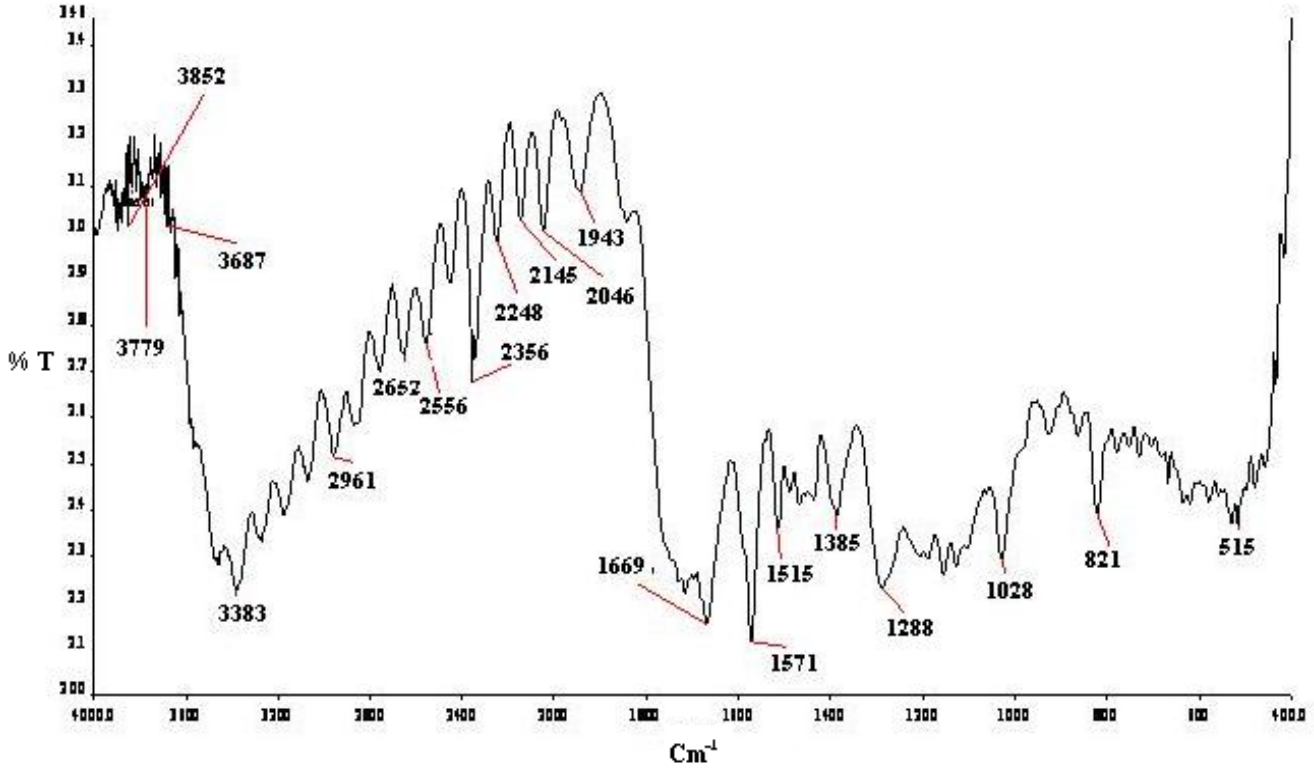
% T
3852
3687
3779
3383
2961
2657
2556
2248
2356
2145
1943
2046
1669
1571
1515
1385
1288
1028
821
515
Cm-1

Fig. S6.

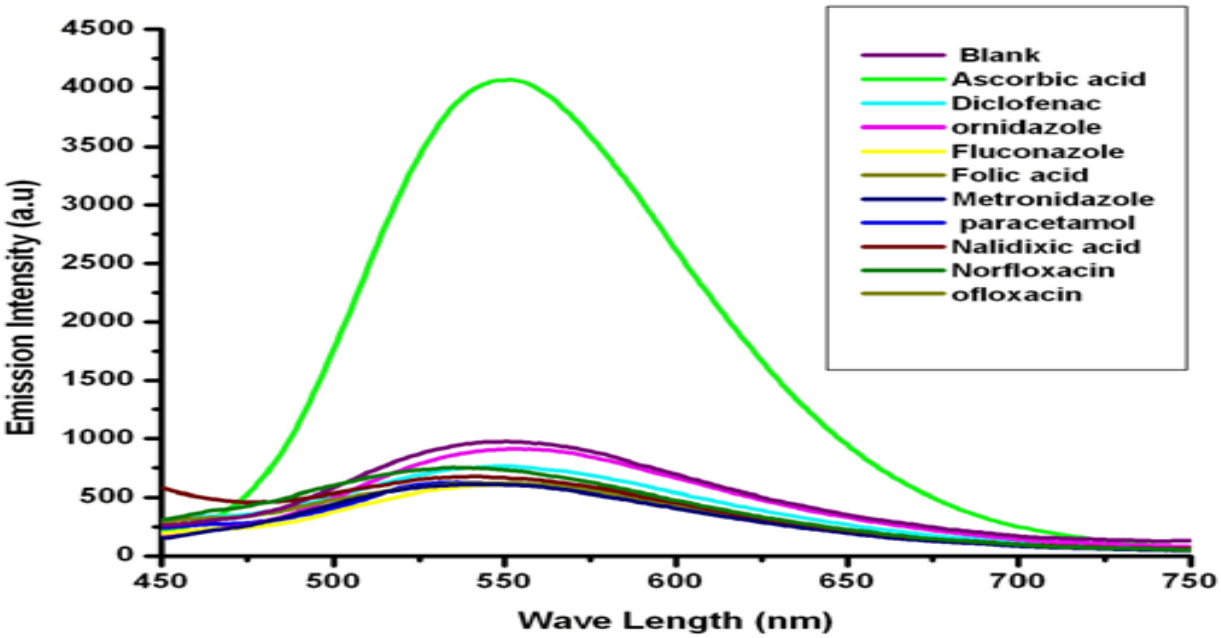
Emission Intensity (a.u)
Wave Length (nm)
Blank
Ascorbic acid
Diclofenac
ornidazole
Fluconazole
Folic acid
Metronidazole
paracetamol
Nalidixic acid
Norfloxacin
ofloxacin

Fig. S7.

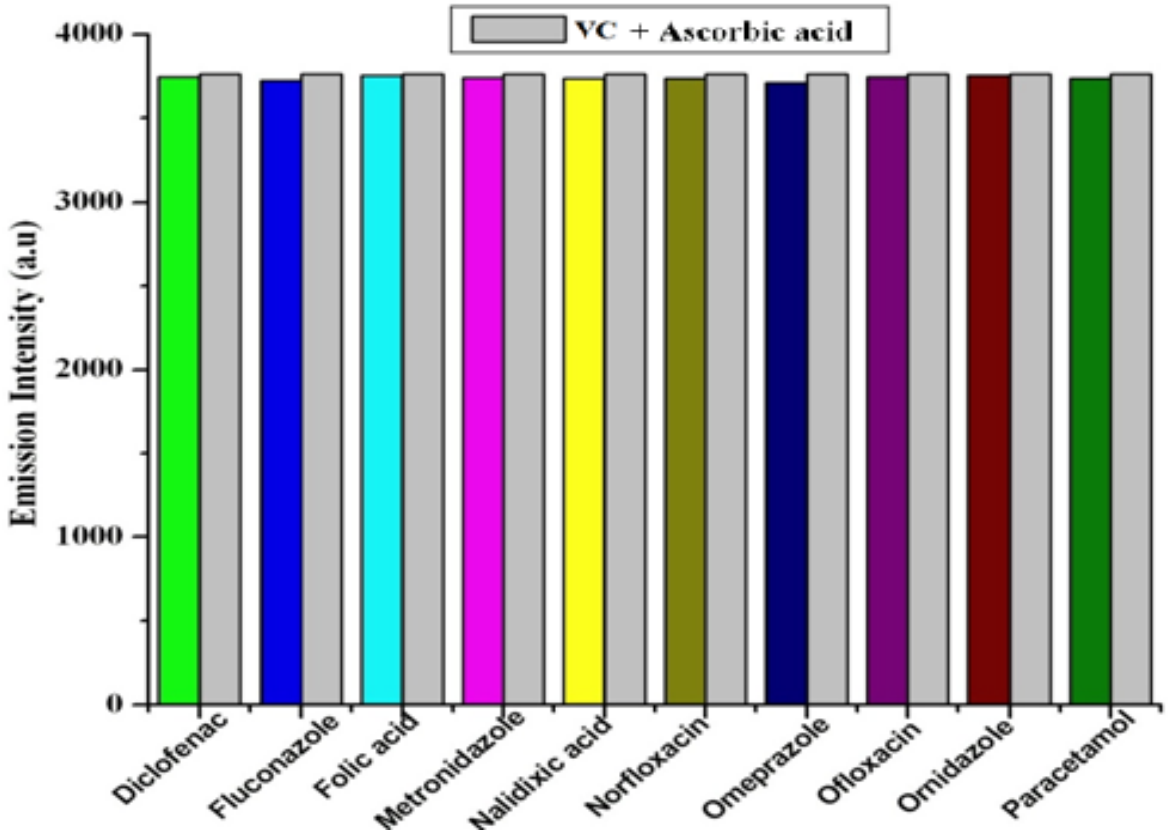
VC + Ascorbic acid
Emission Intensity (a.u)
Diclofenac
Fluconazole
Folic acid
Metronidazole
Nalidixic acid
Norfloxacin
Omeprazole
Ofloxacin
Ornidazole
Paracetamol

Fig. S8.

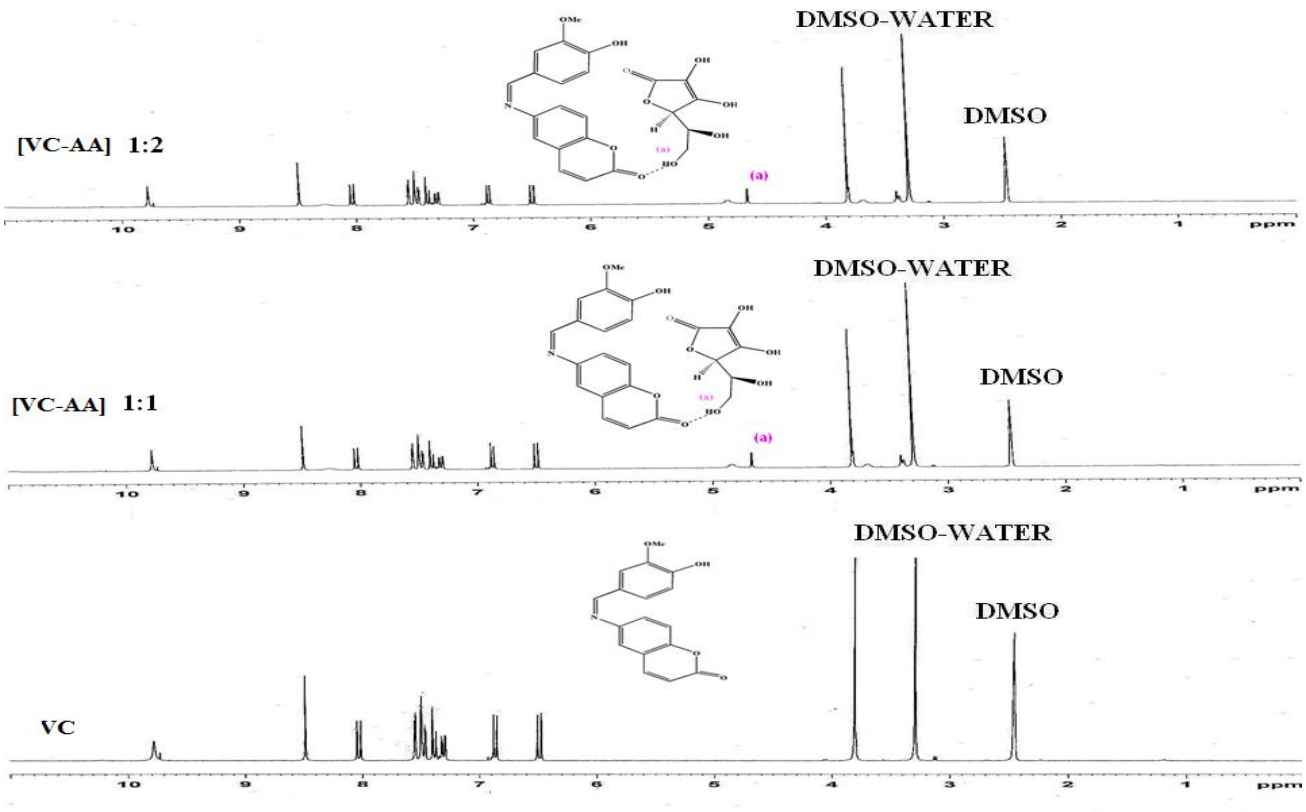

Fig. S9.

Pharmaceutical formulations

The following commercially available common medicines were analyzed. All are purchased from Indian Pharmaceutical Company, India.

(1) Diclofenac tablet®contains 100 mg diclofenac sodium per tablet.

(2) Paracetamol tablet®contains 500 mg paracetamol per tablet.

(3) Celine tablet®contains 500 mg ascorbic acid per tablet.

(4) Folic acid tablet®contains 100 mg folic acid acid per tablet.

(5) Nalidixic acid tablet®contain 500 mg nalidixic acid per tablet.

(6) Ofloxacin tablet ®contains 200 mg ofloxacin per tablet.

(7) Norfloxacin tablet ®contains 500 mg norfloxacin per tablet.

(8) Metronidazole tablet ®contains 200 mg metronidazole per tablet.

(9) Fluconazole tablet ®contains 150 mg fluconazole per tablet.

(10) Ornidazole tablet ®contains 500 mg ornidazole per tablet.

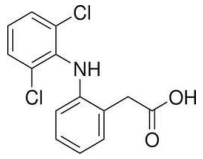

Diclofenac

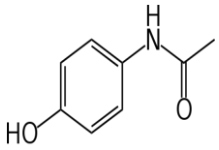

Paracetamol

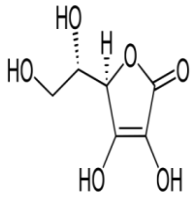

Ascorbic Acid

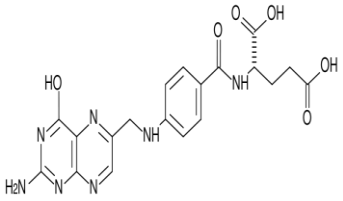

Folic acid

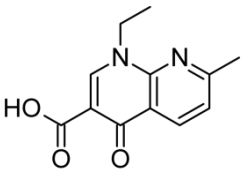

Nalidixic acid

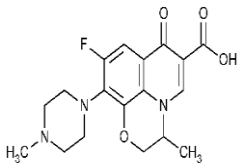

Ofloxacin

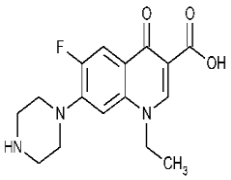

Norfloxacin

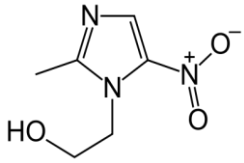

Metronidazole

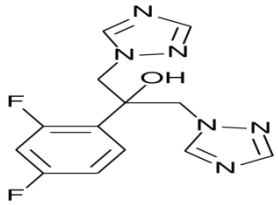

Fluconazole

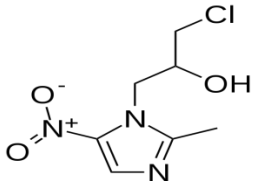

Ornidazole

List of 10 common medicines

Quantum yield measurement

The fluorescence quantum yield of the complex was determined using anthracene as a reference with a known ϕ_R value of 0.27 in methanol.[1]The complex and the reference dye were excited at same wavelength (350 nm), maintaining nearly equal absorbance (0.1) and the emission spectra. The area of the emission spectrum was integrated using the software available in the instrument and the quantum yield is calculated according to the following equation:

$$\phi_S/\phi_R = [A_S / A_R] \times [(Abs)_R /(Abs)_S] \times [\eta_S^2/\eta_R^2] \quad (1)$$

Here, ϕ_S and ϕ_R were the fluorescence quantum yield of the sample and reference respectively. A_S and A_R were the area under the fluorescence spectra of the sample and the reference respectively, $(Abs)_S$ and $(Abs)_R$ were the respective optical densities of the sample and the reference solution at the wavelength of excitation, and η_S and η_R are the values of refractive index for the respective solvent used for the sample and reference.

Reference

1W. H. Melhuish, *J. Phys. Chem.*,1961, **65**, 229.

Table S1. Crystal data and structure refinement for **VC**

Empirical formula	C16 H11 N O3
Formula weight	295.29
Temperature	173(2) K
Wavelength	0.71070 Å

Crystal system	Orthogonal
Space group	Pca21
a, Å	7.0607(2) Å
b, Å	6.6616 (3) Å
c, Å	28.2993(9) Å
α (°)	90
β (°)	90
γ (°)	90
Volume	1331.07(7) $Å^3$
Z	4
Density (calculated)	1.474 Mg/m^3
Absorption coefficient (Mo-Kα radiation)	0.106 mm^{-1}
F(000)	616
Theta range for data collection	0.975 to 26.39°
Reflections collected	2724
Completeness to theta = 25.00°	194.99 %
Max. and min. transmission	0.987 and 0.980
Refinement method	Full-matrix least-squares on F^2
Goodness-of-fit on F^2	0.950
R indices (all data)	R1 = 0.035, wR2 = 0.0840

Table S2. Bond lengths (Å) of **VC**

Atom1	Atom2	Length (A°)	Atom1	Atom2	Length (A°)
C1	C2	1.404	C4	C5	1.390
C1	C6	1.396	C5	C6	1.379
C1	C8	1.464	C5	H5	0.950
C10	H10	0.951	C6	H6	0.950
C11	H11	0.950	C7	H7B	0.980
C11	C12	1.385	C7	H7C	0.981
C11	C10	1.376	C7	H7A	0.979
C12	C16	1.396	C8	H8	0.950
C14	H14	0.950	C9	C10	1.406
C14	C13	1.444	N1	C8	1.288
C15	C16	1.448	N1	C9	1.416
C15	C14	1.345	O1	C7	1.437
C15	H15	0.950	O1	C3	1.372
C17	C16	1.396	O2	H2O	0.824
C17	C9	1.386	O2	C4	1.358
C17	H17	0.950	O3	C12	1.382
C2	H2	0.950	O3	C13	1.378
C3	C2	1.376	O4	C13	1.214
C3	C4	1.401			

Table S3. Bond angles (^{0}) of **VC**

C3—O1—C7	116.60(14)	H7A—C7—H7C	109.500
C4—O2—H2O	107.8(19)	H7B—C7—H7C	109.500
C13—O3—C12	121.57(15)	C6—C5—C4	120.05(17)
C6—C1—C2	119.57(17)	C6—C5—H5	120.000
C6—C1—C8	122.66(17)	C4—C5—H5	120.000
C2—C1—C8	117.67(16)	C14—C15—C16	120.21(17)
O1—C3—C2	125.34(16)	C14—C15—H15	119.900
O1—C3—C4	114.17(16)	C16—C15—H15	119.900
C2—C3—C4	120.47(18)	C17—C16—C12	118.83(16)
C3—C2—C1	119.74(17)	C17—C16—C15	123.52(17)
C3—C2—H2	120.100	C12—C16—C15	117.64(17)
C1—C2—H2	120.100	C17—C9—C10	118.84(16)
C8—N1—C9	116.26(16)	C17—C9—N1	119.20(16)
C9—C17—C16	120.44(16)	C10—C9—N1	121.93(16)
C9—C17—H17	119.800	C5—C6—C1	120.46(18)
C16—C17—H17	119.800	C5—C6—H6	119.800
C10—C11—C12	118.26(17)	C1—C6—H6	119.800
C10—C11—H11	120.900	N1—C8—C1	123.55(17)
C12—C11—H11	120.900	N1—C8—H8	118.200
O2—C4—C5	119.20(17)	C1—C8—H8	118.200
O2—C4—C3	121.10(17)	C15—C14—C13	121.60(17)
C5—C4—C3	119.69(17)	C15—C14—H14	119.200
O3—C12—C11	116.89(17)	C13—C14—H14	119.200
O3—C12—C16	121.32(17)	C11—C10—C9	121.75(18)
C11—C12—C16	121.79(17)	C11—C10—H10	119.100
O1—C7—H7A	109.500	C9—C10—H10	119.100
O1—C7—H7B	109.500	O4—C13—O3	116.48(16)
H7A—C7—H7B	109.500	O4—C13—C14	125.88(18)
O1—C7—H7C	109.500	O3—C13—C14	117.65(16)

Table S4. Torsional angles (^{0}) of **VC**

C7—O1—C3—C2	-19.2(3)	C11—C12—C16—C15	-179.8(2)
C7—O1—C3—C4	159.07(16)	C14—C15—C16—C17	178.65(19)
O1—C3—C2—C1	179.30(16)	C14—C15—C16—C12	-0.4(3)
C4—C3—C2—C1	1.1(3)	C16—C17—C9—C10	-3.3(3)
C6—C1—C2—C3	-0.1(3)	C16—C17—C9—N1	178.89(17)
C8—C1—C2—C3	-176.58(17)	C8—N1—C9—C17	-143.14(19)
O1—C3—C4—O2	-1.3(2)	C8—N1—C9—C10	39.2(3)
C2—C3—C4—O2	177.12(17)	C4—C5—C6—C1	-0.9(3)
O1—C3—C4—C5	179.66(17)	C2—C1—C6—C5	0.0(3)
C2—C3—C4—C5	-2.0(3)	C8—C1—C6—C5	176.26(18)
C13—O3—C12—C11	179.74(18)	C9—N1—C8—C1	-174.20(17)

C13—O3—C12—C16	0.1(3)	C6—C1—C8—N1	2.5(3)
C10—C11—C12—O3	179.10(17)	C2—C1—C8—N1	178.82(19)
C10—C11—C12—C16	-1.2(3)	C16—C15—C14—C13	1.1(3)
O2—C4—C5—C6	-177.28(19)	C12—C11—C10—C9	-0.9(3)
C3—C4—C5—C6	1.8(3)	C17—C9—C10—C11	3.2(3)
C9—C17—C16—C12	1.3(3)	N1—C9—C10—C11	-179.09(19)
C9—C17—C16—C15	-177.80(17)	C12—O3—C13—O4	-179.70(17)
O3—C12—C16—C17	-179.28(17)	C12—O3—C13—C14	0.5(3)
C11—C12—C16—C17	1.1(3)	C15—C14—C13—O4	179.1(2)
O3—C12—C16—C15	-0.2(3)	C15—C14—C13—O3	-1.1(3)

Applications

The biosensor was applied for determination of level of ascorbic acid in fruit juices and vitamin C tablets.

Ascorbic acid determination in fruit juices

The contents of L-ascorbic acid in fruits/vegetables (Orange, lemon, guava, grape apple, strawberry, beans (green) and tomato) juices were determined by fluorescence method and compared with the reference method[43]. The results are given in Table 1. Ascorbic acid content in vitamin C tablets as measured by the present sensor was 51.49 mg dl^{-1} in Lemon, 48.54 mg dl^{-1} in Orange, 36.05 mg dl^{-1} in Grape and 7.13 mg dl^{-1} in Apple.

Ascorbic acid determination in vitamin C tablets

Ascorbic acid content in vitamin C tablets as measured by the present sensor was 497.2 mg/tablet in Lamcea and 194.0 mg/tablet in Becozyme C forte (multivitamin tablet). The results are represented in Table 2.

Table 1. Ascorbic acid determination in fruit juices

Fruit/vegetable juice	**AA** concentration measured by reference method[43] (mg dl^{-1})[a] (Mean ± S.D.)	**AA** concentration measured by fluorescence method with **VC** (mg dl^{-1})[a] (Mean ± S.D.)	Relative SD (%) of proposed method
Lemon	51.33 ± 1.15	51.49 ± 1.92	3.73
Orange	48.33 ± 2.88	48.54 ± 2.29	4.72
Grape	34.75 ± 1.38	36.05 ± 2.11	5.85
Apple	7.00 ± 1.00	7.13 ± 1.19	16.69

[a] Mean value of three replications.

Table 2. Ascorbic acid determination in vitamin C tablets

Table	**[VC-AA]** (mg/tablet)	**[VC-AA]** conc. measured by reference method[43] (mg/tablet)[a]		**[VC-AA]** conc. by Fluorescence method mg/tablet)[a]	
		Mean±S.D	RSD(%)	Mean±S.D	RSD(%)
Lamcea	500	496.3 ± 1.52	0.306	497.2 ± 1.29	0.259
Becozyme c forte (multivitamin)	200	192.7 ± 1.52	0.78	194.0 ± 1.47	0.758

[a] Mean value of three replications.

43 N. Chauhan, J. Narang and C. S. Pundir, *Analyst*, 2011, **136**, 1938